

Improvements in Spiral-Bevel Gears to Reduce Noise and Increase Strength

David G. Lewicki and Robert F. Handschuh
Vehicle Propulsion Directorate
U.S. Army Research Laboratory
Lewis Research Center
Cleveland, Ohio

Zachary S. Henry
Bell Helicopter Textron, Inc.
Fort Worth, Texas

and

Faydor L. Litvin
University of Illinois at Chicago
Chicago, Illinois

Prepared for the
1994 International Gearing Conference
sponsored by the University of Newcastle Upon Tyne
Tyne, England, September 7-9, 1994



National Aeronautics and
Space Administration

DTIC
ELECTE
FEB 01 1995
S G D

19950131 005



DISTRIBUTION STATEMENT A

Approved for public release;
Distribution Unlimited

IMPROVEMENTS IN SPIRAL-BEVEL GEARS TO REDUCE NOISE AND INCREASE STRENGTH

David G. Lewicki and Robert F. Handschuh
Vehicle Propulsion Directorate
U.S. Army Research Laboratory
Lewis Research Center
Cleveland, Ohio 44135

Zachary S. Henry
Bell Helicopter Textron, Inc.
Fort Worth, Texas 76101

Faydor L. Litvin
University of Illinois at Chicago
Chicago, Illinois 60680

DTIC TAB		<input checked="" type="checkbox"/>
Unannounced		<input type="checkbox"/>
Justification		
By		
Distribution /		
Availability Codes		
Dist	Avail and/or Special	
A-1		

SYNOPSIS Advanced-design spiral-bevel gears were tested in an OH-58D helicopter transmission using the NASA 500-hp Helicopter Transmission Test Stand. Four different gear designs were tested. The four designs tested were the current design of the OH-58D transmission, a higher-strength design the same as the current but with an increased fillet radius to reduce gear tooth bending stress, and two versions of a lower-noise design the same as the high-strength but with modified tooth geometry to reduce transmission error and noise. Noise, vibration, and tooth strain tests were performed and significant gear stress and noise reductions were achieved.

1 INTRODUCTION

Spiral-bevel gears are used extensively in rotorcraft applications to transfer power and motion through non-parallel shafts. Even though spiral-bevel gears have had considerable success in these applications, they are a main source of vibration in gearboxes, and thus, a main source of noise in cabin interiors (1,2).

Various investigators have studied spiral-bevel gears and their influence on vibration and noise (3,4,5). Most studies show that transmission error, defined as the difference in relative motion of an output gear with respect to the input pinion, is the major contributor to undesirable vibration and noise. A common practice is to modify spiral-bevel gear surface topology to permit operation in a misaligned mode to compensate for housing deflections. Over compensation for this type of operation, however, leads to large transmission error and higher noise and vibration levels.

In this study, gears with tooth surfaces designed for reduced transmission errors using methods of Litvin and Zhang (3) were manufactured and tested. Also as part of this study, gears with tooth fillet and root modifications to increase strength were manufactured and tested. By increasing these radii, reduced stresses were achieved, and thus, increased strength. Tooth fillet radii larger than those on current gears were made possible by recent advances in spiral-bevel gear grinding technology (6). Advanced gear grinding was achieved through redesign of a current gear grinder and the addition of computer numerical control.

The objective of this report is to describe the results of the experiments to evaluate advanced spiral-bevel gear designs. The work was part of a joint project in support of the U.S. Army/NASA Advanced Rotorcraft Transmission

(ART) program (7,8). Experimental tests were performed on the OH-58D helicopter main-rotor transmission in the NASA 500-hp Helicopter Transmission Test Stand. The baseline OH-58D spiral-bevel gear design, two versions of a low-noise design, and a high-strength design were tested. Noise, vibration, and tooth strain test results are presented.

2 APPARATUS

2.1 OH-58D main-rotor transmission

The OH-58 Kiowa is a U.S. Army single-engine, light, observation helicopter. The OH-58D is an advanced version developed under the U.S. Army Helicopter Improvement Program (AHIP). The OH-58D main-rotor transmission is shown in Fig. 1. It is currently rated at maximum continuous power of 346 kW (464 hp) at 6016 rev/min input speed, with the capability of 10 second torque transients to 485 kW (650 hp), occurring once per hour, maximum. The main-rotor transmission is a two-stage reduction gearbox with an overall reduction ratio of 15.23:1. The first stage is a spiral-bevel gear set with a 19-tooth pinion that meshes with a 62-tooth gear. Triplex ball bearings and one roller bearing support the bevel-pinion shaft. Duplex ball bearings and one roller bearing support the bevel-gear shaft. Both pinion and gear are straddle-mounted.

2.2 Spiral-bevel test gears

Four different spiral-bevel gear designs were tested. The first design tested was the baseline and used the current geometry of the OH-58D design. Table 1 lists basic design parameters. The reduction ratio of the bevel set is 3.26:1. All gears were made using standard aerospace practices where the surfaces were carburized and ground. The material used for all test gears was X-53 (AMS 6308).

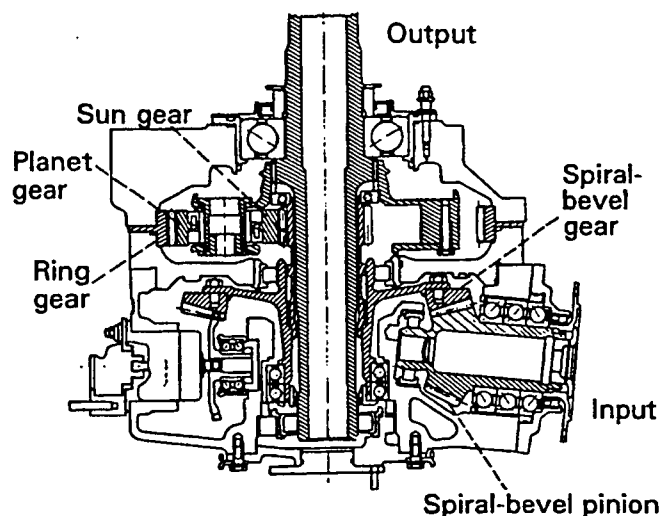


Fig 1. OH-58D helicopter main-rotor transmission.

Table 1. Baseline spiral-bevel gear parameters of the OH-58D main-rotor transmission.

Number of teeth,	
pinion	19
gear	62
Module, mm (diametral pitch, in ⁻¹)	4.169 (6.092)
Pressure angle, deg	20
Mean spiral angle, deg	35
Shaft angle, deg	95
Face width, mm (in.)	36.83 (1.450)

The second spiral-bevel design tested was an increased strength design. The configuration was identical to the baseline except that the tooth fillet radius of the pinion, x_p , was doubled (Fig. 2). Also, the tooth fillet radius of the gear, x_g , was slightly increased (to $1.16 x_g$) and made full fillet.

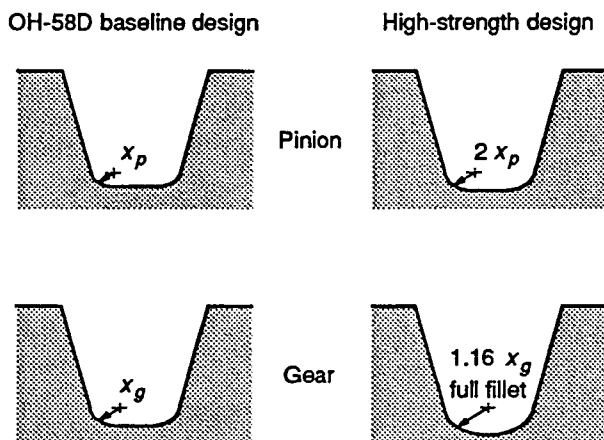


Fig 2. Comparison of OH-58D and high-strength spiral-bevel gear designs.

The third spiral-bevel design tested was a low-noise design. The low-noise design was identical to the increased-strength design except the pinion was slightly altered to reduce transmission error. The gear member was unchanged. The low-noise design was based on the idea of local synthesis that provided at the mean contact point the following conditions of meshing and contact (3): a) the required gear ratio and its derivative, b) the desired direction of the tangent to the contact path, and c) the desired orientation and size of the major axis of the instantaneous contact ellipse. The local synthesis was complemented with a tooth contact analysis (3). Using this approach, the machine tool settings for reduced noise were determined. As with the high-strength design, precise control of the manufactured tooth surfaces were made possible by advances in the final grinding operation machine tool (6). Fig. 3 shows a topological comparison between a low-noise and baseline spiral-bevel pinion tooth. The dotted lines are the baseline tooth datum and the solid lines are the measured difference in topology of a low-noise gear compared to the baseline. Solid lines above the dotted plane indicate an addition of material (compared to the baseline) and lines below the plane indicate a removal. The effect of the topological change in the low-noise design was a reduction in overall crowning of the tooth, leading to an increase in contact ratio and reduced transmission error.

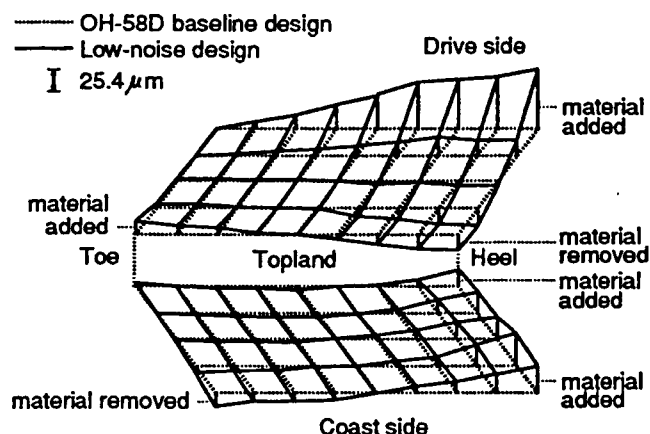


Fig 3. Topological comparison of OH-58D and low-noise spiral-bevel pinions.

The fourth design tested was a modified version of the low-noise design. The fourth design was identical to the third but had slightly more stock removed in the flank portion of the pinion tooth to prevent interference with the top of the gear member during operation. The stock removal was achieved by a decrease in the pressure angle at the tip of the grinding wheel used on the pinion during final machining.

2.3 Test procedure

The OH-58D transmission was tested in the NASA Lewis 500-hp helicopter transmission test stand (1). Two sets of the baseline design, two sets of the high-strength design, two sets of the low-noise design, and one set of the modified low-noise design were tested. Noise and vibration

tests were performed on all sets of each design. Tests were performed at 100-percent transmission input speed (6016 rev/min) and torques of 50, 75, 100, and 125-percent of maximum design. The transmission oil inlet temperature was set at 99 °C (210 °F). The oil used conformed to a DOD-L-85734 specification. In addition to the noise and vibration tests, one set of each of the baseline, high-strength, and low-noise designs were instrumented with strain gages and tested. Strain tests were not performed on the modified low-noise design.

For the noise tests, acoustic intensity measurements were performed using the two-microphone technique. The microphones used had a flat response (± 2 dB) up to 5000 Hz and a nominal sensitivity of 50 mV/Pa. The microphones were connected to a spectrum analyzer which computed the acoustic intensity from the imaginary part of the cross-power spectrum. Near the input region of the OH-58D transmission, a grid was installed which divided the region into sixteen areas (Fig. 4). The acoustic intensity was measured at the center of each of the sixteen areas. Only positive acoustic intensities (noise flowing out of the areas) were considered. The acoustic intensities were then added together and multiplied by the total area of the grids to obtain sound power of the transmission input region.

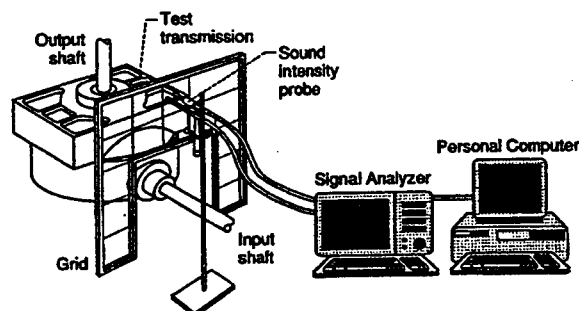


Fig. 4. Sound intensity measurement system.

For the vibration tests, ten piezoelectric accelerometers were mounted at various locations on the OH-58D transmission housing (Fig. 5). The accelerometers were located near the input spiral-bevel area (accelerometers 1, 2, and 10, measuring radially to the input shaft), the ring gear area (3, 4, and 9, measuring radially to the planetary), and on the top cover (5 through 8, measuring vertically). Accelerometers 1 through 8 had a 1 to 25,000-Hz (± 3 dB) response, 4 mV/g sensitivity, and integral electronics. Accelerometers 9 and 10 had a 2 to 6000-Hz (± 5 percent) response and required charge amplifiers.

The vibration tests were performed in conjunction with the noise tests. The acoustic intensity data were collected on-line during testing while the vibration data were recorded on tape and processed off-line. The vibration data were later analyzed using time averaging. Here, the vibration data recorded on tape were input to a signal analyzer along with a tach pulse from the transmission input shaft. The signal analyzer was triggered from the tach pulse to read

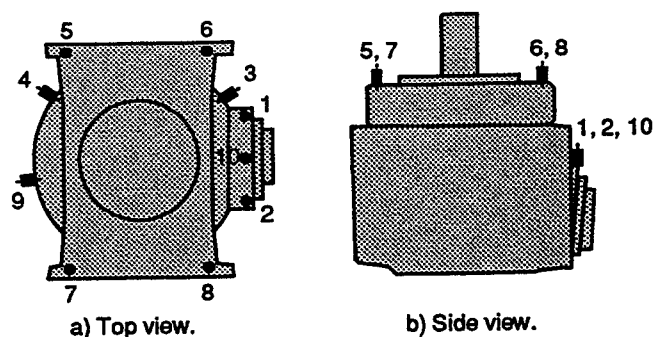
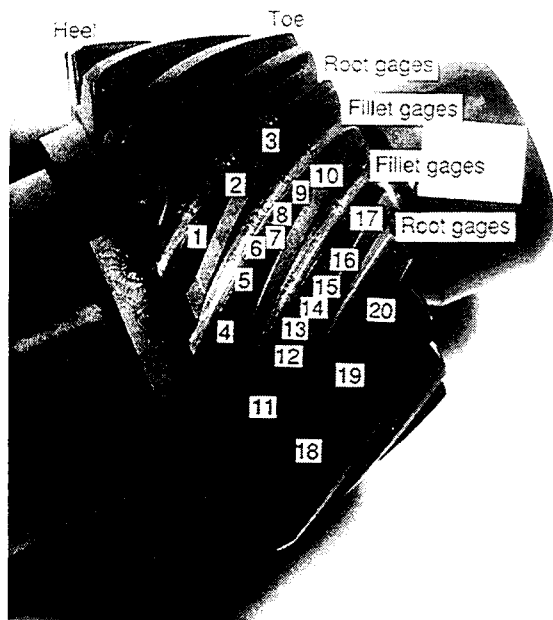


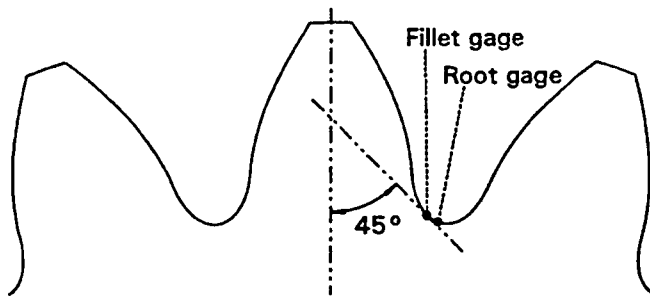
Fig. 5. Accelerometer locations of OH-58D transmission.

the vibration data when the transmission input shaft was at the same position. The vibration signal was then averaged in the time domain using 100 averages. This technique removed all the vibration which was not synchronous to the input shaft. Before averaging, the major tones in the vibration spectrum of the OH-58D baseline design were the spiral-bevel and planetary gear fundamental frequencies and harmonics. Time averaging removed the planetary contribution, leaving the spiral-bevel contribution for comparing the different design configurations.

For the strain tests, twenty strain gages were mounted on the spiral-bevel pinions and twenty-six gages were mounted on the spiral-bevel gears of one set of each of the baseline, high-strength, and low-noise designs (Fig. 6). Gages were positioned evenly across the tooth face widths with some in the fillet area and some in the root area of the teeth. The fillet gages were placed on the drive side of the teeth, at a point on the tooth cross-section where a line at a 45° angle with respect to the tooth centerline intersected the tooth profile (Fig. 6b). The fillet gages were placed there to measure maximum tooth bending stress. Previous studies on spur gears showed that the maximum stresses were at a line 30° to the tooth centerline (9). 45° was chosen for the current tests to minimize the possibility of the gages being destroyed due to tooth contact. In addition to maximum tensile stresses, root stresses can become significant in lightweight, thin-rimmed aerospace gear applications (10). Thus, root gages were centered between teeth in the root to measure gear rim stress. Tooth fillet and root gages were placed on successive teeth to determine loading consistency. The grid length of the gages was 0.381 mm (0.015 in) and the nominal resistance was 120 Ω . The gages were connected to conditioners in a Wheatstone bridge circuit using a quarter-bridge arrangement. Static strain tests were performed on both the spiral-bevel pinions and gears. Dynamic strain tests were performed only on the spiral-bevel pinions since a slip ring assembly was not available for the gear.



a) Gage numbering.



b) Cross-sectional view.

Fig 6. Strain gage locations on spiral-bevel pinion.

3 RESULTS AND DISCUSSION

3.1 Noise tests

The dominant spikes in the noise spectrum for the baseline design were the spiral-bevel and planetary meshing frequencies. The effect of torque on sound power is given in Fig. 7. The sound power was found by summation of the spiral-bevel meshing frequency (1905 Hz) and second harmonic (3810 Hz). The baseline and high-strength designs produced basically the same noise since the difference between them was in the tooth fillet geometry. There was some scatter in the baseline and high-strength results due to manufacturing tolerances of the different sets and assembly tolerances. The low-noise and modified low-noise designs produced a significant decrease in spiral-bevel gear noise compared to the baseline and high-strength designs. To further investigate the effect of assembly tolerances, the tests on set 1 of the low-noise design were repeated. The gears were completely disassembled and reassembled in the transmission, and the tests were repeated

two additional times. The results showed the same trend and were repeatable to within about 2 dB. At 100-percent torque, the noise due to the spiral-bevel mesh was 11 to 21 dB lower than that of the baseline and high-strength designs. Also, a decrease in noise was most prevalent at 100 and 125-percent torque and less prevalent at 50 and 75-percent torque.

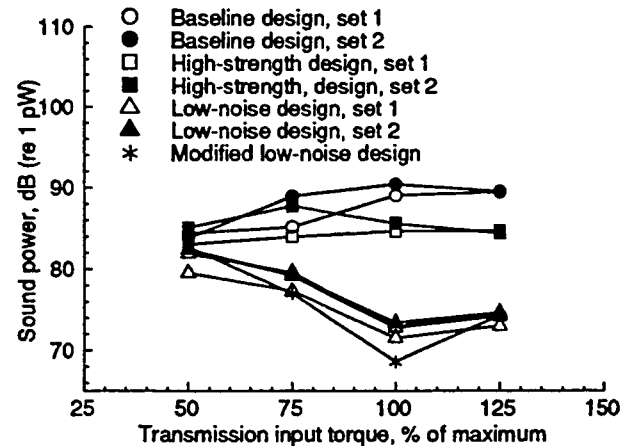


Fig 7. Sound power of spiral-bevel frequencies.

3.2 Vibration tests

There was a significant reduction in spiral-bevel gear vibration for the low-noise and modified low-noise designs. The effect of torque on vibration for accelerometer 1 is given in Fig. 8. Shown in the figure is time-averaged acceleration processed up to 10,000 Hz. The results were root-mean-square (rms) calculations of the averaged time-domain signals. Since the time-averaging removed vibration non-synchronous to the input shaft, the results in Fig. 8 were basically the cumulation of the spiral-bevel meshing frequency (1905 Hz) and second through fifth harmonics.

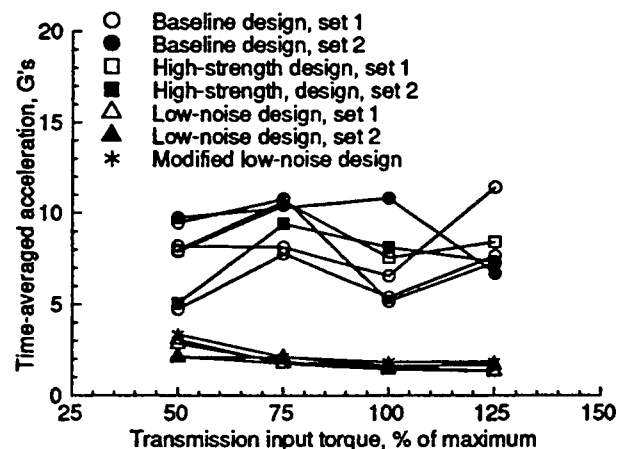


Fig 8. Accelerometer 1, input bevel housing.

As with the noise measurements, the vibration for the baseline and high-strength designs were similar with some scatter. Again, the figure clearly shows a significant reduction in spiral-bevel gear vibration for the low-noise and modified low-noise designs compared to the baseline and high-strength designs. Like the noise results, the

reduction in vibration was greater at the higher torques (100 and 125 percent). The results of the other nine accelerometers were similar. From the results of all ten accelerometers and at 100-percent torque, the vibration for the low-noise design due to the spiral-bevel mesh was on the average 4 to 10 g's lower than that of the baseline and high-strength designs.

3.3 Strain tests

A typical result of the static strain tests for the spiral-bevel pinion fillet gages is shown in Fig. 9. The data were from tests at 100-percent torque. Shown in the figure are the fillet stresses of two successive strain-gaged teeth at the same face width location. The high-strength design produced a significant reduction in tensile stress and a slight increase in compressive stress compared to the baseline. For tests at 100-percent torque, the maximum tensile stress of the pinion fillet for the high-strength design was on the average 27-percent lower than that of the baseline design. The low-noise design exhibited a "widening" of the stress-position curve and a reduction in the peak tensile and peak compressive stress. The reduction in stress was a result of the increased tooth fillet radius and also the increased contact ratio due to the modified tooth geometry. The maximum tensile stress of the pinion fillet for the low-noise design was on the average 31-percent lower than that of the baseline.

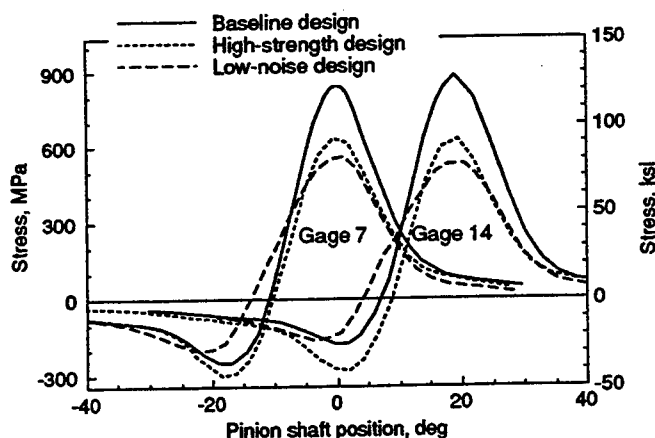


Fig 9. Spiral-bevel pinion fillet strain gage results for static strain tests at 100-percent torque.

The results for the spiral-bevel pinion root gages (not shown) produced a significant increase in the compressive root stress for the high-strength and low-noise designs compared to the baseline. This was believed to be due to the removal of material for the increased fillet, thus lowering the rim thickness. For the spiral-bevel gear fillet gages, there was a slight decrease in the peak tensile stresses for the high-strength and low-noise designs compared to the baseline for gage locations away from the ends of the teeth. Also, the stress levels of the gear were significantly lower to those of the pinion. The maximum tensile and compressive root stresses of the gear were slightly higher for the high-strength design compared to the baseline. The gear root stresses were similar for the

baseline and low-noise design.

A typical stress-time waveform from the dynamic strain tests for a spiral-bevel pinion fillet gage (gage 6) at 100-percent torque is shown in Fig. 10. R is defined as $\sigma_{min}/\sigma_{max}$, σ_{mean} is the mean stress $(=\sigma_{max}+\sigma_{min})/2$, and σ_{alt} is the alternating stress $(=\sigma_{max}-\sigma_{min})/2$. The waveform shows very similar characteristics to that of the static strain tests. No detrimental dynamic loads were discovered for any of the designs (one possible reason could be the moderate speed of the mesh, 6016 rev/min pinion speed). The maximum tensile stress peaks varied approximately ± 3 percent (one standard deviation). As with the static tests, the results from the dynamic tests showed a significant reduction in the tensile stresses for the high-strength and low-noise designs.

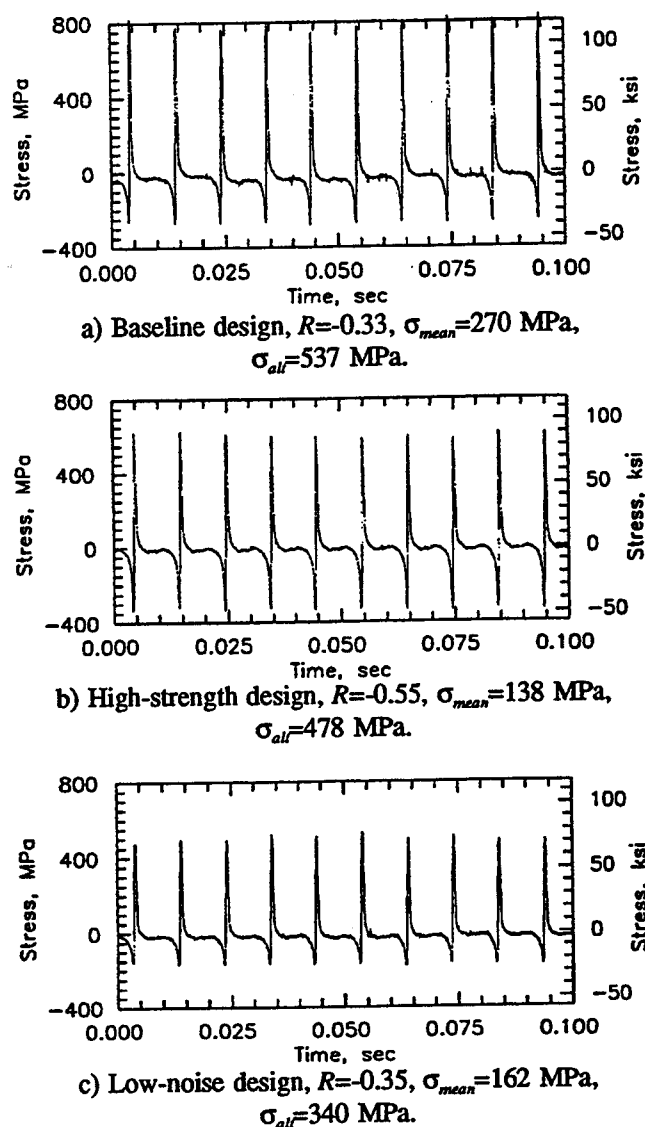


Fig 10. Spiral-bevel pinion gage 6 dynamic strain results.

The maximum tensile and compressive stress during contact from all the working pinion strain gages of the dynamic tests at 100-percent torque were compiled (Fig. 11). The maximum tensile stress of the high-strength design was on the average 22-percent lower than the baseline. The maximum tensile stress of the low-noise design was on the average 28-percent lower.

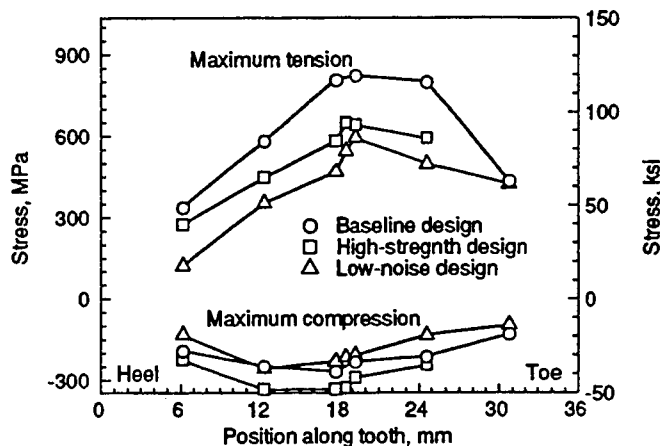


Fig 11. Stresses along tooth face width; dynamic strain tests, spiral-bevel pinion fillet gages, 100-percent torque.

3.4 Visual inspection

From visual inspection, the contact pattern for both the baseline and high-strength designs was typical for aerospace spiral-bevel gears. The pattern was along the full width of the tooth and tapered to an elliptical contour center on the pitch line at the toe and heel. The contact pattern for the low-noise and modified low-noise designs was significantly different. Full contact along the top edge of the tooth occurred with no contact approximately 5 mm from the edge of the heel. The pinions of the low-noise design had a "hardline" in the flank area of the tooth about 30 mm in length and 0.25 mm in width (a hardline is defined as a concentrated wear line usually on the tooth flank (at start of pinion contact) or tooth tip (at end of pinion contact) caused by interference of the pinion and gear during operation). The pinion of the modified low-noise design also had a hardline in the flank area, but it was significantly smaller than that of the low-noise design. Its dimensions were about 23 mm in length and 0.12 mm in width. It was apparent that the modified low-noise design required a slightly greater amount of removal in the flank area in order to eliminate the hardline condition.

4 CONCLUSIONS

Advanced-design spiral-bevel gears were tested in an OH-58D helicopter transmission using the NASA 500-hp Helicopter Transmission Test Stand. Four different gear designs tested included the current design of the OH-58D transmission, a higher-strength design with a modified tooth fillet, and two versions of a lower-noise design with modified tooth topology. The following results were obtained:

1. A significant decrease in spiral-bevel gear noise and vibration was achieved with the low-noise design. For tests at 100-percent speed and torque, an 11 to 21-dB reduction in noise and a 4 to 10 g reduction in vibration was obtained.

2. A significant reduction in maximum tensile stress was achieved with the high-strength and low-noise designs. For tests at 100-percent speed and torque, a 22-percent reduction in maximum dynamic tensile stress was obtained with the high-strength design and a 28-percent reduction was obtained with the low-noise design.

3. A hardline condition was present in the pinion tooth flank area of the first version of the low-noise design. Removal of material in the second version of the low-noise design reduced the hardline condition although additional removal of material is required to eliminate the condition.

5 REFERENCES

- (1) Lewicki, D.G., and Coy, J.J., Vibration Characteristics of OH-58A Helicopter Main Rotor Transmission, 1987, NASA TP-2705, AVSCOM TR-86-C-42.
- (2) Mitchell, A.M., Oswald, F.B., and Coe, H.H., Testing of UH-60A Helicopter Transmission in NASA-Lewis 2240-kW (3000-hp) Facility, 1986, NASA TP-2626.
- (3) Litvin, F.L., and Zhang, Y., Local Synthesis and Tooth Contact Analysis of Face-Milled Spiral Bevel Gears, 1991, NASA CR-4342, AVSCOM TR-90-C-28.
- (4) Gosselin, C., Cloutier, L., and Brousseau, J., Tooth Contact Analysis of High Conformity Spiral Bevel Gears, Proceedings of the International Conference on Motion and Power Transmissions, 1991, pp. 725-730.
- (5) Fong, Z.H., and Tsay, C.B., Kinematic Optimization of Spiral Bevel Gears, Journal of Mechanical Design, 1992, Vol. 114, No. 3, pp. 498-506.
- (6) Scott, H.W., Computer Numerical Control Grinding of Spiral Bevel Gears, 1991, NASA CR-187175, AVSCOM TR-90-F-6.
- (7) Bill, R.C., Advanced Rotorcraft Transmission Program, 1990, NASA TM-103276, AVSCOM TR-90-C-015.
- (8) Henry, Z.S., Advanced Rotorcraft Transmission (ART) - Component Test Results, presented at the 28th AIAA/ASME/SAE Joint Propulsion Conference, 1992.
- (9) Hirt, M.C.O., Stress in Spur Gear Teeth and Their Strength as Influenced by Fillet Radius, Ph.D. Dissertation, Technische Universitat Munchen, 1976, translated by the American Gear Manufacturers Association.
- (10) Drago, R.J., Design Guidelines for High-Capacity Bevel Gear Systems, AE-15 Gear Design, Manufacturing and Inspection Manual, Society of Automotive Engineers, 1990, pp. 105-121.

REPORT DOCUMENTATION PAGE			Form Approved OMB No. 0704-0188	
Public reporting burden for this collection of information is estimated to average 1 hour per response, including the time for reviewing instructions, searching existing data sources, gathering and maintaining the data needed, and completing and reviewing the collection of information. Send comments regarding this burden estimate or any other aspect of this collection of information, including suggestions for reducing this burden, to Washington Headquarters Services, Directorate for Information Operations and Reports, 1215 Jefferson Davis Highway, Suite 1204, Arlington, VA 22202-4302, and to the Office of Management and Budget, Paperwork Reduction Project (0704-0188), Washington, DC 20503.				
1. AGENCY USE ONLY (Leave blank)		2. REPORT DATE May 1994		3. REPORT TYPE AND DATES COVERED Technical Memorandum
4. TITLE AND SUBTITLE Improvements in Spiral-Bevel Gears to Reduce Noise and Increase Strength			5. FUNDING NUMBERS WU-505-62-10 1L162211A47A	
6. AUTHOR(S) David G. Lewicki, Robert F. Handschuh, Zachary S. Henry, and Faydor L. Litvin				
7. PERFORMING ORGANIZATION NAME(S) AND ADDRESS(ES) NASA Lewis Research Center Cleveland, Ohio 44135-3191 and Vehicle Propulsion Directorate U.S. Army Research Laboratory Cleveland, Ohio 44135-3191			8. PERFORMING ORGANIZATION REPORT NUMBER E-8896	
9. SPONSORING/MONITORING AGENCY NAME(S) AND ADDRESS(ES) National Aeronautics and Space Administration Washington, D.C. 20546-0001 and U.S. Army Research Laboratory Adelphi, Maryland 20783-1145			10. SPONSORING/MONITORING AGENCY REPORT NUMBER NASA TM-106613 ARL-TR-459	
11. SUPPLEMENTARY NOTES Prepared for the 1994 International Gearing Conference, University of Newcastle Upon Tyne, England, September 7-9, 1994. David G. Lewicki and Robert F. Handschuh, Vehicle Propulsion Directorate, U.S. Army Research Laboratory, Lewis Research Center, Cleveland, Ohio; Zachary S. Henry, Bell Helicopter Textron, Inc., Fort Worth, Texas 76101; and Faydor L. Litvin, University of Illinois at Chicago, Chicago, Illinois 60680. Responsible person, David G. Lewicki, organization code 2730, (216) 433-3970.				
12a. DISTRIBUTION/AVAILABILITY STATEMENT Unclassified - Unlimited Subject Category 37			12b. DISTRIBUTION CODE	
13. ABSTRACT (Maximum 200 words) Advanced-design spiral-bevel gears were tested in an OH-58D helicopter transmission using the NASA 500-hp Helicopter Transmission Test Stand. Four different gear designs were tested. The four designs tested were the current design of the OH-58D transmission, a higher-strength design the same as the current but with an increased fillet radius to reduce gear tooth bending stress, and two versions of a lower-noise design the same as the high-strength but with modified tooth geometry to reduce transmission error and noise. Noise, vibration, and tooth strain tests were performed and significant gear stress and noise reductions were achieved.				
14. SUBJECT TERMS Transmissions (machine elements); Gears; Noise; Vibration; Strain measurements			15. NUMBER OF PAGES 8	
			16. PRICE CODE A02	
17. SECURITY CLASSIFICATION OF REPORT Unclassified	18. SECURITY CLASSIFICATION OF THIS PAGE Unclassified	19. SECURITY CLASSIFICATION OF ABSTRACT Unclassified	20. LIMITATION OF ABSTRACT	